社団法人　電子情報通信学会
THE INSTITUTE OF ELECTRONICS,
INFORMATION AND COMMUNICATION ENGINEERS

信学技報
TECHNICAL REPORT OF IEICE.

省電力ルータに与える負荷を考慮したエンド間帯域計測手法の提案

小林　大翼†　　長谷川　剛††　　村田　正幸†

† 大阪大学 大学院情報科学研究科　〒 565-0871 大阪府吹田市山田丘 1–5
†† 大阪大学 サイバーメディアセンター　〒 560–0043 大阪府豊中市待兼山町 1–32
E-mail: †{d-kobays,murata}@ist.osaka-u.ac.jp, ††hasegawa@cmc.osaka-u.ac.jp

あらまし　ネットワーク負荷に応じてルータ処理性能やリンク速度の動的な変更を行うことにより、省電力を図る省電力ルータがネットワーク内に存在すると、ネットワーク負荷に応じてエンド端末間パスの物理帯域が変動するため、従来提案されているエンド間利用可能帯域計測手法の計測精度が劣化すると考えられる。また、帯域計測のために発生するネットワーク負荷により、省電力ルータの省電力効果が十分に得られない可能性がある。そこで本稿では、ルータの省電力動作に伴う物理帯域の変動を考慮した、エンド間帯域計測手法を提案する。提案手法は、エンド間物理帯域と利用可能帯域を同時に計測し、利用可能帯域の計測に用いるパケット数を調整することにより、ルータの省電力動作を阻害しない計測を可能にする。シミュレーション結果より、提案手法を用いた場合、従来提案されている利用可能帯域計測手法と同等の計測精度が得られ、ルータの省電力効果を損なわずに計測を行えることを示す。
キーワード　利用可能帯域、物理帯域、帯域計測、省電力、ルータ

End-to-end bandwidth measurement method considering effects on power-saving routers

Daisuke KOBAYASHI†, Go HASEGAWA††, and Masayuki MURATA†

† Graduate School of Information Science and Technology, Osaka University　1–5, Yamadaoka, Suita, Osaka, 565-0871 Japan
†† Cybermedia Center, Osaka University　1–32, Machikaneyama-cho, Toyonaka, Osaka, 560–0043 Japan
E-mail: †{d-kobays,murata}@ist.osaka-u.ac.jp, ††hasegawa@cmc.osaka-u.ac.jp

Abstract　In environment when power-saving routers and switches exist in an end-to-end path, since the amount of bandwidth-related resources of an end-to-end network path changes over time, the accuracy of existing end-to-end measurement methods of available bandwidth may degrade. Furthermore, the energy efficiency of power-saving routers also decreases due to additional traffic load by bandwidth probing. In this report, we propose a method for measuring physical capacity and available bandwidth simultaneously for the situation in which power-saving routers exist on the end-to-end path. By showing simulation results, we show that the proposed method can measure available bandwidth with high accuracy, while maintaining the energy efficiency of power-saving routers.
Key words　Available bandwidth, Physical capacity, Bandwidth measurement, Energy efficiency, Router

1. Introduction

The expectation for power saving for networking equipment has raised because of the increase in the energy consumption associated with ever-intensifying network traffic. To realize energy efficient networking, a number of researchers have focused on technologies that dynamically adjust the processing performance and the link speed of routers and switches according to the network traffic load. For instance, a power saving method for Gigabit Ethernet Passive Optical Network (G-EPON) was introduced [1,2] in which switches adjust their link speed to either 1 Gbps or 10 Gbps and enter sleep mode according to the queue lengths reported from optical network units, by which the current traffic volume can be inferred. A number of studies [3–5] have focused on power saving routers and switches which dynamically control the transmission capacity on the basis of the change in the traffic volume. Moreover, power saving techniques for Ethernet adapters with adaptive link rates [6, 7], ADSL2 and ADSL2+ [8] have also been proposed.

When such routers and switches exist on an end-to-end path, the

amount of bandwidth-related resources of the path changes largely over time since such equipment changes their performance in a short cycle. Therefore, acquiring information on network resources, such as bandwidth-related information, on the path by measurement is important for maintaining the performance of network applications. For measuring end-to-end available bandwidth, numerous tools have been developed, such as Pathload [9], Spruce [10] and others [11–15]. These tools implicitly assume that the physical capacity on the path remain unchanged during the measurement. In other words, these tools do not take into account the existence of power-saving routers on the path. Furthermore, since most measurement methods involve sending many probing packets at an extremely high rate, the energy efficiency of power-saving routers may deteriorate due to the additional traffic load.

In this report, we propose a method for measuring physical capacity and available bandwidth simultaneously for the situation in which power-saving routers exist on the end-to-end path. We first investigate interactions between the measurement by Pathload, which is a popular tool for measuring the end-to-end available bandwidth, and the behavior of power-saving routers. We reveal the measurement accuracy degrades due to fluctuations of physical capacity, as well as deteriorating the energy efficiency of power-saving routers because of the large traffic volume for bandwidth probing. That is, to measure the available bandwidth accurately, the changes in the physical capacity should be observed during the available bandwidth measurement. Therefore, we propose a simultaneously measurement method of physical capacity and available bandwidth. The main feature of the proposed method is adjusting the number of probing packets for the available bandwidth measurement based on the measured physical capacity, to avoid ill-effect on power-saving routers. Moreover, the proposed method continuously measures physical capacity to determine whether or not to stop the progress of the available bandwidth measurement. We conduct simulation experiments to evaluate the performance of the proposed method. We evaluate the measurement accuracy and the effect of the behavior of the proposed measurement tool on the energy efficiency of power-saving routers.

2. Interactions between bandwidth measurement and power-saving routers

In this section we first introduce the available bandwidth measurement algorithm by Pathload and the model for power-saving router used in this paper. We then discuss the interactions between end-to-end bandwidth measurement and power-saving routers.

2.1 Power-saving router model

We refer [16] for constructing the model for the power-saving router which adjust its physical capacity according to its utilization. The power-saving router monitors its link utilization at regular intervals, that are the order of microseconds to milliseconds, and adjusts its physical capacity according to the observed utilization. We define the maximum value of the physical capacity, in other words, the capacity without power saving, as C_{max}. Assuming an N-level stepwise power saving configuration, the i th setting of the physical capacity, denoted as C_i, is defined as follows.

$$C_i = \frac{i}{N} C_{max} (i = 1, \cdots, N) \tag{1}$$

We define τ as the length of the interval for monitoring link utilization and assume that the power-saving router changes the physical capacity at the same interval. We define a *time slot* as time duration divided by the interval. $P(t)$ represents the amount of traffic observed at the link at the t th time slot, and $C(t)$ is the physical capacity at the t th slot. Then, the link utilization at the t th slot, $u(t)$, is represented as follows.

$$u(t) = \frac{P(t)}{C(t)\tau} \tag{2}$$

The average link utilization $U(t)$ at the t th time slot is calculated as an exponential moving average.

$$U(t) = (1 - w)U(t - 1) + wu(t) \tag{3}$$

The parameter w in Eq. (3) is the averaging weight. The power-saving router determines the physical capacity at the (t+1) th time slot according to the following equation.

$$C(t+1) = \begin{cases} C_{i+1} & \text{if } U(t) \geqq \lambda_u \text{ and } i < N \\ C_{i-1} & \text{if } U(t) \leqq \lambda_l \text{ and } i > 1 \\ C_i & \text{otherwise} \end{cases} \tag{4}$$

The parameters λ_u and λ_l in Eq. (4) are thresholds of the link utilization which are used to determine whether the power-saving router should increase or decrease its physical capacity, respectively.

2.2 Pathload algorithm

In this subsection, we explain the measurement procedure of Pathload. For the measurement of the available bandwidth of an end-to-end path between a sender and a receiver, the sender sends packet streams to the receiver at a certain rate. As the receiver observes the intervals at which packets in the streams arrive, it compares the arrival intervals with the corresponding sending intervals. The sender then adjusts the sending rate of subsequent packet streams according to the observation results provided by the receiver. This cycle is repeated until the algorithm obtains an estimate of the available bandwidth. The packet streams sent in every cycle are referred to as a *fleet*.

Pathload maintains upper and lower bounds of search range for the available bandwidth. $r_{max}(f)$ and $r_{min}(f)$ are denoted the upper bound and the lower bound of the search range, respectively, at the f th ($f = 1, \cdots$) cycle. The sender determines $r(f)$, which is the sending rate of a packet stream in the f th cycle, as follows.

$$r(f) = \frac{r_{max}(f) + r_{min}(f)}{2} \tag{5}$$

Pathload updates $r_{max}(f)$ and $r_{min}(f)$ according to whether or not packet streams observed by the receiver have increasing trends of one-way delays, which is determined by using Pairwise Comparison Test (PCT) metric and Pairwise Difference Test (PDT) metric. Here, we define the number of packets in a packet stream as K and one-way delays of the j th packet stream as D_j. Then, PCT metric, denoted as E_{PCT}, is defined as follows.

$$E_{PCT} = \frac{\sum_{j=2}^{K} I(D_j > D_{j-1})}{K - 1} \tag{6}$$

The value of $I(X)$ is one if X is true, and zero otherwise. E_{PCT} ranges between zero and one, and the larger value means the stronger increasing delay trends. PDT metric, denoted as E_{PDT}, is defined as follows.

$$E_{PDT} = \frac{D_K - D_1}{\sum_{j=2}^{K} |D_j - D_{j-1}|} \tag{7}$$

PDT is always equal to or smaller than one, and the larger value means the stronger increasing delay trends. Pathload determines that a packet stream has an increasing delay trend if E_{PCT} higher than 0.55 and E_{PDT} higher than 0.4.

Pathload determines that $r(f)$ is higher than the available bandwidth of the path if 70% or more packet streams in the cycle have increasing delay trends. In contrast, it determines that $r(f)$ is lower the available bandwidth when 70% or more packet streams do not have increasing delay trends. Otherwise, it determines that there is no strict ordering between $r(f)$ and the available bandwidth. Then the sender updates the search range according to the estimation results. Note that A means the actual value of the available bandwidth of the path. To avoid a backlog of the packet streams in the path, Pathload sets the inter-stream latency to $\max(RTT, cV_S(f))$, where RTT is Round Trip Time of the path, $V_S(f)$ is the length of the packet stream in the f th cycle, and c is set to nine.

Pathload terminates the measurement and outputs $r_{max}(f)$ and $r_{min}(f)$ as a measurement result when the width of the search range $(r_{max}(f) - r_{min}(f))$ becomes smaller than ω, which is configured by the user.

2.3 Interactions between bandwidth measurement and power-saving routers

In Pathload, probing packet streams are sent along the end-to-end network path at a rate that corresponds fairly close to the actual available bandwidth. On the other hand, the power-saving router proposed in [16] monitors the link utilization at regular intervals in the order of milliseconds. Therefore, it is expected that the power-saving router changes its physical capacity to accommodate the

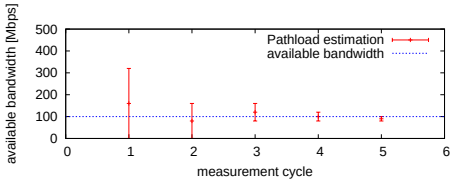

(a) In case of no changes in physical capacity

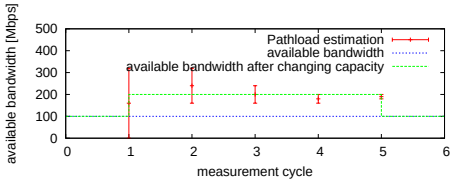

(b) In case of increase in physical capacity after 1 st cycle

図 1 Measurement process of Pathload

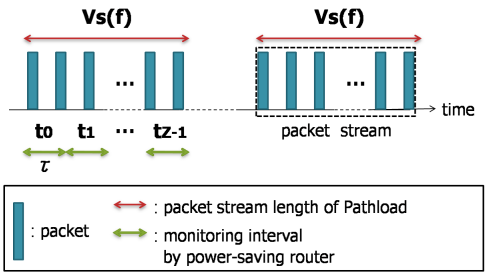

図 2 Relationship between packet stream length and monitoring interval of link utilization

bandwidth probing traffic by Pathload. This behavior brings the following two ill-effects. First, it degrades the energy efficiency of the power-saving routers, meaning that it should not increase its physical capacity to accommodate the bandwidth probing traffic. Second, it also degrades the accuracy of the bandwidth measurement since most of existing bandwidth measurement methods, including Pathload, does not assume the changes in the physical capacity during the measurement procedure.

In what follows we show a brief sample of the latter ill-effect. For that purpose, we show numerical calculation results of Pathload algorithms, assuming that a power-saving router exists on the path. In Figures 1(a) and 1(b), we depict the measurement process of Pathload. In these figures, the vertical axis represents the available bandwidth and the horizontal axis represents the measurement cycle. In both figures, it is assumed that Pathload terminates the measurement procedure with five cycles. The actual value of the available bandwidth is set to 100 Mbps. In Figure 1(a), we assume that the power-saving router does not change its physical capacity during the measurement. In this case, the accurate measurement result can be obtained. On the other hand, in Figure 1(b), we assume the situation where the power-saving router increase its physical capacity at the end of the 1 st cycle, and the available bandwidth based on the increased physical capacity becomes 200 Mbps. We observe that the measured available bandwidth is based on the increased physical capacity, which is not an accurate estimation. Such degradation of the measurement accuracy occurs when the power-saving router increase its physical capacity due to increased traffic load by the measurement itself.

2.4 Conditions for not affecting a power-saving router

We discuss the parameter settings of Pathload which ensure that the behavior of a power-saving router remains unaffected. We assume that the power-saving router has been already configured its physical capacity according to the current traffic load.

Using Eqs. (3) and (4), the conditions for the power-saving router to maintain its physical capacity are as follows.

$$\begin{aligned} U(t) &= (1-w)U(t-1) + wu(t) \\ &= w\sum_{k=1}^{t}(1-w)^{t-k}u(k) \\ &\leqq \lambda_u \end{aligned} \tag{8}$$

We divide $P(t)$, which is the amount of traffic observed at the tight link, into $P^L(t)$ and $P^C(t)$ as follows.

$$P(t) = P_L(t) + P_C(t) \tag{9}$$

where $P^L(t)$ indicates the amount of traffic caused by bandwidth probing, and $P^C(t)$ is the amount of cross traffic. By using Eqs. (2), (3) and (9), the average link utilization $U(t)$ can be rewritten as follows.

$$\begin{aligned} U(t) &= w\sum_{k=1}^{t}(1-w)^{t-k}u(k) \\ &= w\sum_{k=1}^{t}(1-w)^{t-k}\frac{P_L(k)+P_C(k)}{C(t)\tau} \\ &= w\sum_{k=1}^{t}(1-w)^{t-k}\frac{P_L(k)}{C(t)\tau} + \\ &\quad w\sum_{k=1}^{t}(1-w)^{t-k}\frac{P_C(k)}{C(t)\tau} \end{aligned} \tag{10}$$

The first term in Eq. (10) represents traffic contributed by measurement probing, and the second term represents cross traffic. Assuming cross traffic arriving at the link of the power-saving router at a fixed rate r_C, Eq. (10) can be rewritten as follows.

$$U(t) = w\sum_{k=1}^{t}(1-w)^{t-k}\frac{P_L(k)}{C(t)\tau} + \frac{r_C}{C(t)} \tag{11}$$

Then, the spacing between packets, denoted by $T(f)$, is determined as follows by using $r(f)$ and the packet size L.

$$T(f) = \frac{L}{r(f)} \tag{12}$$

In addition, the length of the packet stream in the f th cycle is obtained by using Eq. (12) and K.

$$\begin{aligned} V_S(f) &= KT(f) \\ &= \frac{KL}{r(f)} \end{aligned} \tag{13}$$

In the following discussion, we assume $\tau \leqq V_S(f)$, meaning that the utilization monitoring interval is shorter than the packet stream. The relationship between the packet stream length and the monitoring interval is depicted in Figure 2. The power-saving router monitors the link utilization for time slots $t_0, \ldots, t_{Z-1}$, where $Z = \left\lceil \frac{V_S(f)}{\tau} \right\rceil$. Since the arrival rate of packet steams is closely to the available bandwidth, the link utilization increases considerably, particularly when the packet stream spans multiple monitoring intervals of the link utilization. In this situation, Eq. (8) can be rewritten based on Eq. (11), assuming that the interval between two packet streams is sufficiently large not to affect the calculation of the average link utilization in Eq. (3).

$$\begin{aligned} U(t_{Z-1}) &= w\sum_{k=0}^{Z-1}(1-w)^{Z-1-k}\frac{r(f)}{C(t)} + \frac{r_C}{C(t)} \\ &\leqq \lambda_u \end{aligned} \tag{14}$$

Note that we can control only Z to satisfy Eq. (14), which is achieved by changing K. Therefore, by configuring the number of packets in each packer stream to satisfy Eq. (14), we can prevent Pathload from affecting the behavior of power-saving routers.

3. Simultaneous measurement considering the behavior of power-saving routers

In this section, we propose an end-to-end method for measuring physical capacity and available bandwidth simultaneously. Our

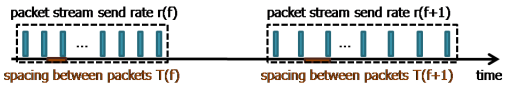

(a) packet stream of Pathload

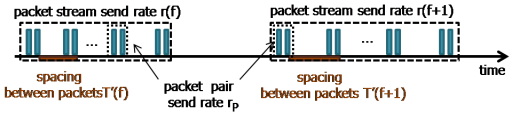

(b) packet stream of the proposed method

図 3 modification of packet streams

proposed method is based on the available bandwidth measurement algorithm by Pathload, and integrate the physical capacity measurement based on CapProbe [17]. We selected CapProbe because it can provide high accuracy and the short measurement time among various tools for measuring physical capacity [13, 14, 18].

3.1 Physical capacity measurement

In CapProbe, the sender host sends a certain number of packet pairs to the receiver host. The receiver host selects the packet pair which has the minimum value of the sum of one-way delays and calculates the physical capacity based on the arrival interval of packets constructing the selected pair. The measurement finishes when one result is obtained.

For the simultaneous measurement in the proposed method, we continue the measurement even after one result is obtained, meaning that the sender host continues sending packet pairs. Then, a new result is given when the packet pair has the one-way delays which is equal to or the smaller than that of the previously selected pair. On the other hand, when a certain number of consecutive packet pairs do not experiences the minimum value of the sum of one-way delays, the sender host reset the measurement since the physical capacity at the power-saving router may change.

3.2 Packet stream for simultaneous measurement

We next explain the constitution of the packet stream, for accommodating measurement procedure of CapProbe. In Figure 3(a), we depict the packet streams in the f th cycle measurement by the original Pathload. The packet stream consists of K packets, each of which has the size of L. The packet inter-spacing $T(f)$ is calculated from the sending rate of packet stream, denoted by $r(f)$, and L. We also depict packet streams of the proposed method in Figure 3(b). We implement the physical capacity measurement by using packet pairs for constructing the packet stream. The packets in the packet stream compose multiple packet pairs, while the number of packets in the packet stream and its total length remain unchanged. We use r_P for representing the sending rate of the packet pair, assuming that r_P is set based on the physical capacity of the link connected to the sender host. We compose $K' = \left\lfloor \frac{K}{2} \right\rfloor$ packet pairs in one packet stream by modifying the packet inter-spacing between the $(2i-1)$ th packet and the $2i$ th packet $(1 \leqq i \leqq K')$ as $\frac{L}{r_P}$.

By this modification to the packet stream we need to change the definition of PCT and PDT as E'_{PCT} and E'_{PDT}, as follows.

$$E'_{PCT} = \frac{\sum_{i=2}^{K'} I(D_{2(i-1)+1} > D_{2(i-1)-1})}{K'-1} \tag{15}$$

$$E'_{PDT} = \frac{D_{K'} - D_1}{\sum_{i=2}^{K'} |D_{2(i-1)+1} - D_{2(i-1)-1}|} \tag{16}$$

3.3 Adjustment of the number of packets for measurement

When we try to prevent the link of the power-saving router from fluctuating the physical bandwidth, adjusting the number of packets in the packet stream based on Eq. (14) is effective. To exploit the equation, we need the following router-related information.

- $C(t)$: the physical capacity of the power-saving router at the t th time slot
- r_C : the amount of cross traffic
- τ : the length of the interval for monitoring the link utilization

When we assume that the physical capacity of the power-saving router is the narrowest in the path, we can use the latest result of the physical capacity measurement as $C(t)$. Moreover, when we also assume that the available bandwidth of the link of the power-saving router is tightest in the path, we can use the difference between measured physical capacity and available bandwidth as r_C. For τ, we use the value presented in [16].

In the f th cycle of the measurement, we configure the number of packets in each packet stream according to Eq. (14) with the measurement results in the previous cycle. We define $K(f)$ as the number of packets in the packet streams in the f th cycle. We limit $K(f) \geqq 4$ since Eqs. (15) and (16) requires more than two packet pairs. We set $K(f)$ to four when valid measurement results are not obtained. Also, we utilized the conservative value for available bandwidth since we should avoid affecting power-saving routers when the measurement of available bandwidth includes significant errors. In detail, we evaluate the confidence intervals of measurement results of available bandwidth and utilize its lower bound as available bandwidth when calculating r_C in Eq. (14).

When $K(f)$ is set to small value, the accuracy of the available bandwidth measurement degrades. For compensating for the degradation, we keep the total number of packets utilized in each measurement cycle. In detail, we set the number of packet streams in the f th cycle, denoted as $M(f)$, as follows.

$$M(f) = \left\lfloor \frac{F}{K(f)} \right\rfloor \tag{17}$$

Note that the parameter F in Eq. (17) is the number of packets in the measurement cycle.

3.4 Statistical processing of measured available bandwidth

Since we assume the continuous measurement of physical capacity and available bandwidth, we can enhance the measurement accuracy by statistical processing of previous measurement results. For available bandwidth we utilize the method in ImTCP [12]. In ImTCP, the sender host calculates $\gamma\%$ confidence interval of the previously measured available bandwidth values and utilize the interval as the initial search range. In the proposed method in this paper, we modify the behavior of the ImTCP in the following two points. First, we round the search range to $2^n\omega$ where n is an integer value. Second, we redesign the extension of the search range when the measurement result can not be found in the initial search range. In detail, when the measurement results indicate the actual available bandwidth falls below the search range, the initial search range of the next measurement, denoted by $[s_{min}^{m+1}, s_{max}^{m+1}]$, is modified as follows.

$$\begin{aligned} s_{min}^{m+1} &= s_{min}^{m} - (s_{max}^{m} - s_{min}^{m}) \\ s_{max}^{m+1} &= s_{max}^{m} \end{aligned} \tag{18}$$

On the other hand, when the measurement results indicate the actual available bandwidth falls above the search range, the initial search range of the next measurement is modified as follows.

$$\begin{aligned} s_{min}^{m+1} &= s_{min}^{m} \\ s_{max}^{m+1} &= s_{max}^{m} + (s_{max}^{m} - s_{min}^{m}) \end{aligned} \tag{19}$$

3.5 Detection of physical capacity fluctuations

By simultaneous measurement of physical capacity and available bandwidth, the changes in physical capacity at the power-saving router can be detected in the available bandwidth measurement. In such cases we should terminate the current measurement procedure of available bandwidth since the measurement accuracy degrades significantly as explained in Subsection 2.3. Furthermore, we should configure the initial search range for the available bandwidth measurement based on the changed physical capacity. Here, B_{bc} and B_{ac} represent the result of the physical capacity measurement before and after changing the result of the measurement, respectively. We calculate the initial search range of the $(m+1)$ th measurement as follows.

$$s_{max}^{m+1} = \begin{cases} \min(s_{max}^{m} + B_{ac} - B_{bc}, r_P) \\ \text{if } (s_{max}^{m} + B_{ac} - B_{bc}) > s_l \\ s_l \qquad \text{otherwise} \end{cases} \tag{20}$$

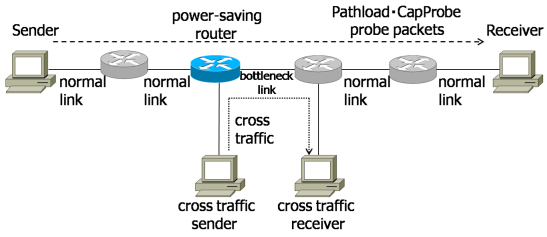

図 4　Network topology for simulation experiments

表 1　Parameters of the power-saving router

Parameter	Variable	Value
Maximum value of physical capacity	C_{max}	1000 Mbps
Number of steps for adjusting physical capacity for adjusting physical capacity	N	10
Upper threshold of link utilization for increasing physical capacity	λ_u	0.8
Lower threshold of link utilization for decreasing physical capacity	λ_l	0.35
Averaging weight	w	0.3
Length of the interval for monitoring link utilization	τ	1 ms

表 2　Parameters of the proposed method

Parameter	Variable	Value
Packet size	L	750 Bytes
Estimate resolution	ω	1 Mbps
Minimum length of the initial search range	s_l	128 Mbps
Confidence interval	γ	95%

$$s_{min}^{m+1} = \begin{cases} \max\left(s_{min}^{m} + B_{ac} - B_{bc}, 0\right) \\ \text{if } \left(s_{min}^{m} + B_{ac} - B_{bc}\right) < r_P - s_l \\ r_P - s_l \qquad \text{otherwise} \end{cases} \tag{21}$$

where s_l represents the minimum length of the initial search range.

4. Evaluation

We conducted simulation experiments to evaluate the performance of the proposed method with the ns-2 network simulator [19]. We first confirm fundamental behaviors of the proposed method. We then observe the effect of the bandwidth measurement by the proposed method on the energy efficiency of the power-saving router.

4.1 Simulation settings

Figure 4 depicts the network topology used in the simulation experiments. We assume that a power-saving router is connected to a bottleneck link, which provides the narrowest physical capacity along the network path between a sender and a receiver. The maximum physical capacity of the bottleneck link is 1000 Mbps. The physical capacity of other links, labeled as normal links in the figure, is 2000 Mbps. The propagation delay of each link is 5 ms. Cross traffic which traverses the bottleneck link from a cross traffic sender to a cross traffic receiver. The packet size of the cross traffic is 1250 Bytes. The half of the cross traffic is generated based on the exponentially-distributed traffic and the rest is based on CBR traffic.

In Tables 1 and 2, we summarize settings of the power-saving router and parameters of the proposed method, respectively. A simulation experiment continues until 100 measurement results are obtained. Each available bandwidth measurement is started as soon as the previous available bandwidth measurement finishes. For each setting we conduct 10 experiments by changing random seeds for generating cross traffic and evaluate their average. In what follows we do not show the evaluation results on the measurement accuracy of physical capacity since the proposed method always give quite accurate measurement results on physical capacity in any parameter settings.

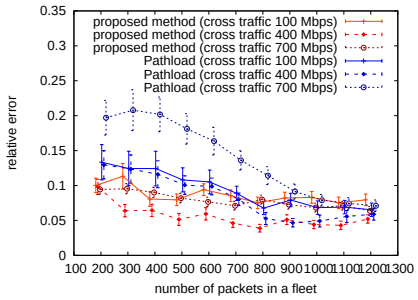

(a) Relative error

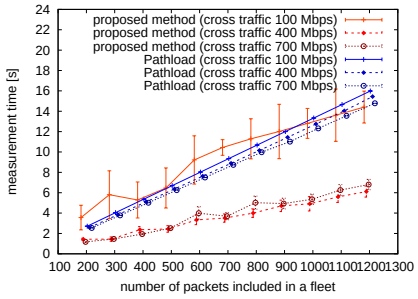

(b) Measurement time

図 5　Results of simulation experiments

4.2 Measurement accuracy and measurement time

We observe the measurement accuracy and the measurement time of the proposed method. Measurement accuracy is evaluated by the relative error, which is defined as $\frac{|A - A'|}{A}$, where A' is the measurement result and A represents the actual available bandwidth. We define the time required for obtaining one available bandwidth measurement as the measurement time. In the evaluation, we focus on the average value of the latter half of results of the measurement. For comparison purposes, we also conduct simulation experiments by using Pathload with default parameters described in [20]. In Pathload simulations, we use a normal router at the bottleneck instead of the power-saving router since the measurement accuracy of Pathload significantly degrades in environment when power-saving routers exist as we described in Subsection 2. 3.

Figures 5(a) and 5(b) plot the accuracy and the measurement time of the available bandwidth measurement with 95% confidence intervals, respectively, as a function of the number of packets in a fleet (F). The amount of cross traffic is set to 100 Mbps, 400 Mbps, and 700 Mbps. From Figure 5(a), we observe that the proposed method outperform the original Pathload, even with the existence of the power-saving router only for the proposed method. In detail, the relative error of almost all measurement results by the proposed method is less than 0.1. Also, the proposed method gives enough accuracy with smaller values of F, while the original Pathload degrades the accuracy when F becomes small. This is because the proposed method utilize previous results for adjusting the initial search range that results in the enough accurate measurement with small number of probe packets.

From Figure 5(b), we observe the measurement time of the proposed method is almost the same as the original Pathload when the amount of the cross traffic is set to 100 Mbps. However, when the amount of the cross traffic is set to 400 Mbps and 700 Mbps, the measurement time of the proposed method becomes less than the original Pathload. This is because the number of packet streams is changed according to previous measurement results. When the amount of the cross traffic is set to 100 Mbps, the available bandwidth becomes smaller than others. Therefore, the measurement time is larger than others due to increasing the number of packet streams. Figure 5(b) shows the measurement times of the original Pathload are not different among three different amounts of the cross traffic. This is why the fixed number of packet streams is sent for obtaining a result in the original Pathload.

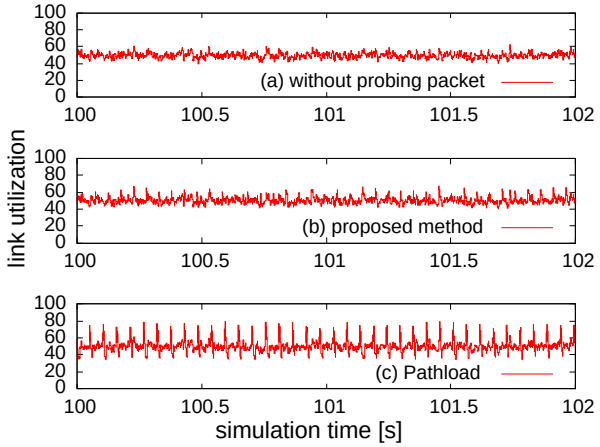

図 6　Fluctuation in the link utilization of the power-saving router

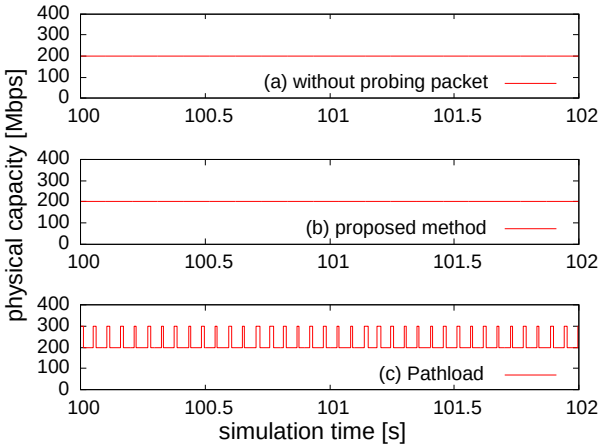

図 7　Fluctuation in the physical capacity of the power-saving router

4.3 Effect on behaviors of the power-saving router

Figures 6 and 7 show the average link utilization and the physical capacity between 100 s and 102 s of the simulation experiments, which has one available bandwidth measurement. We set the amount of the cross traffic to 100 Mbps and $F = 200$. Unlike results in Figure 4.2, we used the power-saving router in the experiment of the original Pathload for investigating the effect of the Pathload measurement on the power-saving router. Figures 6(a) and 7(a) show results in case that the bandwidth measurement is not conducted. From Figure 6(b), when we measure the bandwidth by the proposed method, the fluctuation of the average link utilization is similar to the fluctuation showed in Figure 6(a). In this case, the power-saving router does not increase its physical capacity as we showed in Figure 7(b). From Figure 6(c), the measurement of the original Pathload causes the large fluctuation in the average link utilization due to probe packets. Figure 7(c) shows the power-saving router increased its physical capacity when every packet streams of the original Pathload passed the bottleneck link.

5. Conclusion

In this report, we first described interactions between Pathload and the behavior of power-saving routers and showed that both the measurement accuracy and the energy efficiency of power-saving routers degrade. Then, we proposed a method for measuring physical capacity and available bandwidth simultaneously for the situation in which power-saving routers exist on the end-to-end path. Simulation experiments showed the proposed method could measure available bandwidth with high accuracy, while maintaining the energy efficiency of power-saving routers.

In future work, we plan to enhance the proposed method to measure not only the available bandwidth based on decreased physical capacity of power-saving router, but also the available bandwidth based on maximum physical capacity during power-saving.

文　献

[1] J. Zhang and N. Ansari, “Toward energy-efficient 1G-EPON and 10G-EPON with sleep-aware MAC control and scheduling,” IEEE Communications Magazine, vol.49, no.2, pp.33–38, Feb. 2011.

[2] L. Valcarenghi, D.P. Van, and P. Castoldi, “How to save energy in Passive Optical Networks,” Proceedings of ICTON 2011, pp.1–5, June 2011.

[3] Y. Fukuda, T. Ikenaga, and Y. Oie, “Dynamic transmission capacity control schemes for power saving using a mixture of the history and the latest information,” Proceedings of IEEE GLOBECOM 2010, pp.1438–1442, Dec. 2010.

[4] H. shengWang, L. shiuanPeh, and S. Malik, “A power model for routers: Modeling alpha 21364 and infiniband routers,” IEEE MICRO, vol.23, no.1, pp.26–35, Jan. 2003.

[5] M. Yamada, T. Yazaki, N. Matsuyama, and T. Hayashi, “Power efficient approach and performance control for routers,” Proceedings of IEEE ICC 2009, pp.1–5, June 2009.

[6] F. Blanquicet and K. Christensen, “An initial performance evaluation of rapid PHY selection (RPS) for energy efficient ethernet,” Proceedings of IEEE LCN 2007, pp.223–225, Oct. 2007.

[7] C. Gunaratne, K. Christensen, B. Nordman, and S. Suen, “Reducing the energy consumption of ethernet with Adaptive Link Rate (ALR),” IEEE Transactions on Computers, vol.57, no.4, pp.448–461, April 2008.

[8] G. Ginis, “Low-power modes for ADSL2 and ADSL2+,” White paper, Broadband Communications Group, Texas Instruments, Jan. 2005.

[9] M. Jain and C. Dovrolis, “End-to-End available bandwidth: Measurement methodology, dynamics, and relation with TCP throughput,” Proceedings of ACM SIGCOMM 2002, pp.295–308, July 2002.

[10] J. Strauss, D. Katabi, and F. Kaashoek, “A measurement study of available bandwidth estimation tools,” Proceedings of ACM SIGCOMM 2003, pp.39–44, Nov. 2003.

[11] V.J. Ribeiro, R.H. Riedi, R.G. Baraniuk, J. Navratil, and L. Cottrell, “pathChirp: Efficient available bandwidth estimation for network paths,” Proceedings of ACM PAM 2003, pp.1–11, April 2003.

[12] C.L.T. Man, G. Hasegawa, and M. Murata, “ImTCP: TCP with an inline measurement mechanism for available bandwidth,” Computer Communications Journal special issue of Monitoring and Measurements of IP Networks, vol.29, no.10, pp.2469–2479, June 2006.

[13] R.L. Carter and M.E. Crovella, “Measuring bottleneck link speed in packet-switched networks,” Technical report, Boston University Computer Science Department, March 1996.

[14] A. Downey, “Using pathchar to estimate Internet link characteristics,” Proceedings of ACM SIGCOMM 1999, pp.241–250, Oct. 1999.

[15] Pchar. available at http://www.ca.sandia.gv/ bmah/Software/pchar.

[16] K. Zaitsu, K. Yamamoto, Y. Kuroda, K. Inoue, S. Ata, and I. Oka, “Hardware implementation of fast forwarding engine using standard memory and dedicated circuit,” Proceedings of IEEE ICECS 2010, pp.379–382, Dec. 2010.

[17] R. Kapoor, L. jyhChen, A. N, M. Gerla, and M.Y. Sanadidi, “CapProbe: a simple and accurate capacity estimation technique,” Proceedings of ACM SIGCOMM 2004, pp.67–78, Aug. 2004.

[18] C. Dovrolis, P. Ramanathan, and D. Moore, “Packet-dispersion techniques and a capacity-estimation methodology,” IEEE/ACM Transactions on Networking, vol.12, no.6, pp.963–977, Dec. 2004.

[19] The VINT Project, “Ucb/lbnl/vint network simulator - ns (version 2).”. available at http://www.isi.edu/nsnam/ns/.

[20] M. Jain and C. Dovrolis, “Pathload: A measurement tool for End-to-End available bandwidth,” Proceedings of ACM PAM 2002, pp.14–25, May 2002.